Smart Structures and Systems, Vol. 8, No. 4 (2011) 399-412
DOI: http://dx.doi.org/10.12989/sss.2011.8.5.399

Energy-balance assessment of shape memory alloy-based seismic isolation devices

O.E. Ozbulut* and S. Hurlebaus

Zachry Department of Civil Engineering, Texas A&M University, College Station, TX, USA

(Received January 21, 2011, Revised May 15, 2011, Accepted August 5, 2011)

Abstract. This study compares the performance of two smart isolation systems that utilize superelastic shape memory alloys (SMAs) for seismic protection of bridges using energy balance concepts. The first isolation system is a SMA/rubber-based isolation system (SRB-IS) and consists of a laminated rubber bearing that decouples the superstructure from the bridge piers and a SMA device that provides additional energy dissipation and re-centering capacity. The second isolation system, named as superelastic-friction base isolator (S-FBI), combines the superelastic SMAs with a flat steel-Teflon bearing rather than a laminated rubber bearing. Seismic energy equations of a bridge structure with SMA-based isolation systems are established by absolute and relative energy balance formulations. Nonlinear time history analyses are performed in order to assess the effectiveness of the isolation systems and to compare their performance. The program RSPMatch 2005 is employed to generate spectrum compatible ground motions that are used in time history analyses of the isolated bridge. Results indicate that SRB-IS produces higher seismic input energy, recoverable energy and base shears as compared to the S-FBI system. Also, it is shown that combining superelastic SMAs with a sliding bearing rather than rubber bearing significantly reduce the amount of the required SMA material.

Keywords: shape memory alloy; superelasticity; energy balance; seismic isolation; bridges.

1. Introduction

During strong earthquakes, substantial amounts of energy are imparted to the structures, which may lead to excessive deformations and failure. This input energy should be dissipated through either inherent damping mechanism of the structures or inelastic deformation in order to avoid collapse. Since the bridge structures usually have very low inherent damping, they can experience large deformations to dissipate the seismic input energy relying on inelastic deformations when subjected to strong ground motions. This may cause severe damage or complete collapse as occurred during the past earthquakes (Bruneau 1998, Hsu and Fu 2004, Liu 2009). Bridges are lifelines of the transportation network. Failure of bridges during an earthquake will increase travel time and distance within the network. Therefore, indirect economic loss can also reach to significant levels besides the direct loss resulting from bridge damage (Enke *et al*. 2008).

Seismic isolation has been one of the most commonly used methods to minimize the damaging effects of strong ground motions over past decades. Seismic isolation aims to reduce earthquake energy that enters to the structure by providing flexible interfaces which decouple the support of a

*Corresponding Author, Dr., E-mail: ozbulute@tamu.edu

structure from the horizontal motions of the ground. During an earthquake loading, the seismic isolation (i) reduces the lateral forces in the superstructure by elongating the fundamental period of the structure and dissipating energy and (ii) concentrates the lateral displacements at the isolation level, i.e. limits the structural deformations.

Since an energy-based design method was introduced by Housner (1956), energy-based concepts have been considerably used in the earthquake resistant design of structures (Soong and Constantinou 1994, Constantinou and Reinhorn 1995, Casciati and Lagorio 1996). The basic idea in the energy-based design is that the *energy demand* during a seismic excitation should be less than the *energy supply* of a structural system. In view of energy-based concepts, in seismic isolation, the goal is to reduce the seismic input energy to the system and dissipate the input energy through damping mechanisms. Therefore, an optimal isolation system should minimize the energy transmitted to the structure while dissipating the most of the energy through nonlinear hysteretic deformations in the isolation device with only a small amount of left energy that can cause damage on the main structural system (Austin and Lin 2004).

Several researchers have proposed smart isolation systems which combine smart materials with conventional bearings (Nezhad *et al*. 2008, Usman *et al*. 2009, Ismail *et al.* 2009, Ismail *et al.* 2010). Shape memory alloys (SMAs) are a unique class of metal alloys that have the ability to recover extensive deformations upon removal of the external load (Hurlebaus and Gaul 2006). Superelastic SMAs have hysteretic energy dissipation capacity, excellent re-centering ability and substantial resistance to fatigue and corrosion. Due to their appealing characteristics, superelastic SMAs have been considered as an isolation component by a number of researchers to develop a smart isolation system (Wilde *et al*. 2000, Dolce *et al.* 2007, Attanasi *et al*. 2009, Ozbulut and Hurlebaus 2010a). An innovative SMA-based isolation device in which a sliding system is coupled with inclined CuAlBe SMA bars for energy dissipating and re-centering purposes is introduced by Casciati *et al.* (2007) and Casciati and Faravelli (2009). In another study, Casciati *et al.* (2009) investigated the performance of the developed SMA isolation device for a seismically-excited highway bridge benchmark problem. It was found that the SMA isolation device can largely reduce peak displacement response while increasing peak base shear and overturning moment.

Ozbulut and Hurlebaus (2011a) studied the performance of a superelastic-friction base isolator (S-FBI) that combines a flat sliding bearing and a superelastic SMA device. They identified the optimum design parameters of the S-FBI system for seismic protection of bridges against near-field earthquakes. As an alternative to conventional rubber isolators, Ozbulut and Hurlebaus (2011b) evaluated the performance of a smart rubber bearing system with shape memory alloys. In particular, they explored the effectiveness of SMA/rubber-based isolation systems (SRB-IS) in mitigating response of the bridge structures subjected to near-field earthquakes by performing a sensitivity analysis. Although both the S-FBI system and SRB-IS have been found to be an effective isolation system when their design parameters are judiciously selected, further work is needed to compare the efficiency of these two SMA-based isolation systems.

The goal of this study is to compare the effectiveness of two different SMA-based isolation systems, namely the S-FBI system and SRB-IS, by conducting nonlinear time history analyses with energy balance assessment. Both isolation systems employ a superelastic SMA device that provides a re-centering mechanism and absorbs seismic energy through hysteresis of SMA elements. The S-FBI system combines the SMA device with a steel-Teflon sliding bearing that filters out the earthquake forces, while the SRB-IS integrates the SMA device with a laminated rubber bearing that decouples the superstructure from the bridge piers. Here, the energy balance equations for an

isolated bridge structure are introduced first. Both absolute and relative energy formulations are considered and the relevance of using them for the seismic evaluation of structures subjected to various earthquakes is discussed. Then, the efficacies of the S-FBI system and SRB-IS for seismic protection of bridges are assessed through the results of extensive numerical simulations.

2. Energy-balance equations for an isolated bridge

2.1 Modeling of isolated bridge

A three-span continuous bridge is selected for the numerical simulations (Wang *et al*. 1998). The bridge has a total length of 90 m, and each pier is 8 m tall as shown in Fig. 1. The masses of the deck and each pier are 771.1×10^3 kg and 39.3×10^3 kg, respectively. The moment of inertia of piers and Young's modulus of elasticity are given as 0.64 m^4 and 20.67×10^9 N/m^2, respectively. The fundamental period of non-isolated bridge is 0.45 s. Since the isolation systems installed at the abutment and pier have similar characteristics and therefore, the seismic response of the bridge at the abutment and pier have the same trend, only an internal span is modeled.

A two-degree-of-freedom model of the isolated bridge with the S-FBI system and SRB-IS is shown in the Fig. 1. The S-FBI system utilizes a superelastic SMA device and a flat steel-Teflon bearing, whereas the SRB-IS combines the SMA device with a laminated rubber bearing rather than a sliding bearing. The SMA device simply consists of multiple loops of superelastic Nickel-Titanium (NiTi) wires wrapped around low-friction wheels. The pier is assumed to remain linear-

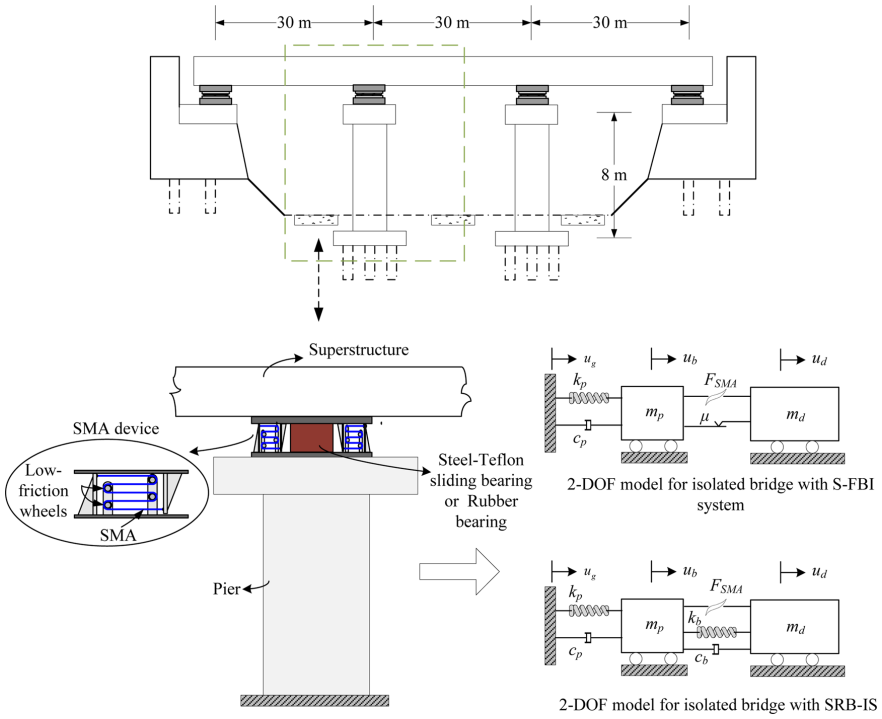

Fig. 1 Model of isolated bridge structure

elastic and modeled with a linear spring and dashpot. The restoring force of the S-FBI system is given as

$$F_{SFBI} = F_f + F_{SMA} \tag{1}$$

where F_f and F_{SMA} denote the frictional resistance force of the steel-Teflon sliding bearings and the nonlinear force of the SMA device, respectively. A hysteretic model is used to simulate the force of the sliding bearings (Constantinou *et al*. 1990). The frictional force at a sliding interface is given by

$$F_f = \mu \cdot W \cdot Z \tag{2}$$

where μ represents the coefficient of friction, W is the normal load carried by the bearing interface, and Z is a hysteretic dimensionless quantity computed from following equation

$$Y\dot{Z} + \gamma|\dot{u}_b||Z||Z|^{n-1} + \beta\dot{u}_b|Z|^n - \dot{u}_b = 0 \tag{3}$$

where Y is the yield displacement of the sliding bearing chosen as 0.0005 m and, γ, β, and n are dimensionless parameters that control the shape of the hysteretic curve and have the values of 0.9, 0.1 and 1, respectively.

It is essential to have a reliable model to capture highly nonlinear behavior of SMAs in numerical simulations. It is known that the temperature and loading frequency considerably affect the mechanical response of SMAs (Ozbulut *et al.* 2007, Casciati and van der Eijk 2008, Casciati and Marzi 2010). In a recent study, Carreras *et al.* (2011) suggested the use case-specific numerical material models to account the influence of various parameters on the behavior of SMAs. Here, a neuro-fuzzy model developed by Ozbulut and Hurlebaus (2010b) is used to simulate the rate- and temperature-dependent force-displacement behavior of the SMA device.

Neuro-fuzzy modeling refers creating a fuzzy inference system (FIS) that is trained by a learning algorithm based on neural networks. The FIS maps an input space to an output space by means of fuzzy if-then rules. Adaptive neuro-fuzzy inference system (ANFIS) is a soft computing approach that employs neural network strategies to develop a fuzzy inference system whose parameters cannot be predetermined (Jang 1993). Due to its ability to create models for dynamic and nonlinear systems in the absence of accurate mathematical models, the FIS and ANFIS has been used in various structural control applications (Casciati and Yao 1995, Casciati *et al.* 1996, Faravelli and Yao 1996). Ozbulut and Hurlebaus (2010b) used the ANFIS to create a simple but an accurate model of superelastic SMA wires. First, a large set of data obtained from tensile tests on NiTi wires with a diameter of 1.5 mm is concatenated to form training, checking and validation data sets for ANFIS simulation. Then, an initial FIS with three input variables that are strain, strain rate and temperature, and a single output that is stress on the wire is created. Each input is fuzzified by defining membership functions. Also, twelve if-then rules are defined to map the input variables to the output. These initial membership function and rules are randomly generated and adjusted by ANFIS during a procedure called training. Once the optimized FIS is obtained, it is validated by a new set of data that has not been used during training.

The restoring force developed in the SRB-IS is given by

$$F_{SRB} = c_b\dot{u}_b + k_b u_b + F_{SMA} \tag{4}$$

where c_b and k_b are the viscous damping and initial stiffness of the laminated rubber bearing; $\dot{u}_b$ and u_b are the velocity and deformation of the bearing, respectively; and F_{SMA} is the force of the SMA device.

2.2 Ground motions used in the analyses

An evaluation of the earlier works related to selection of real ground motion records used in dynamic analyses points out that the spectral shape is the most important ground motion characteristic in modification of real records (Iervolino *et al*. 2009). The program RSPMatch 2005 adjusts real accelerograms in time domain using wavelets to provide a good match with a target response spectrum (Hancock *et al*. 2006). The use of RSPMatch 2005 also significantly reduces the number of records required to achieve a robust estimate of structural response in the engineering analysis (Hancock *et al*. 2008).

In this study, the program RSPMatch 2005 is used to modify the selected historical time histories. A target response spectrum is constructed as per the International Building Code (IBC, 2000) for a site in southern California, U.S.A. assuming firm rock conditions (Malhotra *et al*. 2003). Four ground motion records, namely, 1940 El Centro, 1992 Landers, 1992 Erzincan, 1999 Kocaeli are chosen as seed accelerograms. Fig. 2 shows the target response spectrum used in the analysis and response spectra of selected ground motions for 5% damping level before and after spectral matching. Fig. 3 shows the acceleration and velocity time histories of the spectrally matched records. There is a significant reduction in the spectral misfit after the modification of the records with RSPMatch 2005.

2.3 Absolute and relative energy equations of isolated bridge

The equation of motion of a seismically isolated bridge structure is given as

$$\mathbf{M}\{\ddot{\mathbf{u}}_t(t)\} + \mathbf{C}\{\dot{\mathbf{u}}_t(t)\} + \mathbf{F}_r(t) = 0 \tag{5}$$

where $\{\mathbf{u}_t(t)\}$, $\{\dot{\mathbf{u}}_t(t)\}$ and $\{\ddot{\mathbf{u}}_t(t)\}$ are the vector of absolute displacement, velocity and acceleration of the system, $\{\mathbf{u}_t(t)\}$, $\{\dot{\mathbf{u}}_t(t)\}$ and $\{\ddot{\mathbf{u}}_t(t)\}$ are the vector of relative displacement, velocity and acceleration of the system, $\mathbf{M}$ = (2×2) diagonal mass matrix, $\mathbf{C}$ = (2×2) damping matrix, and $\mathbf{F}_r(t)$ =

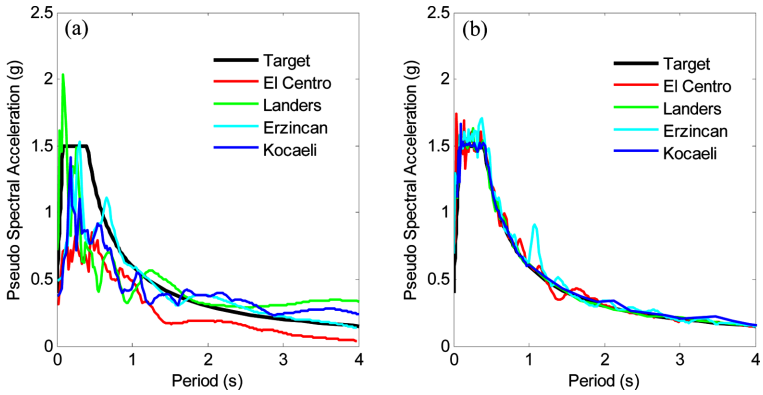

Fig. 2 Target response spectrum compared to response spectra of selected ground motions (a) before and (b) after RSPMatch 2005 modification

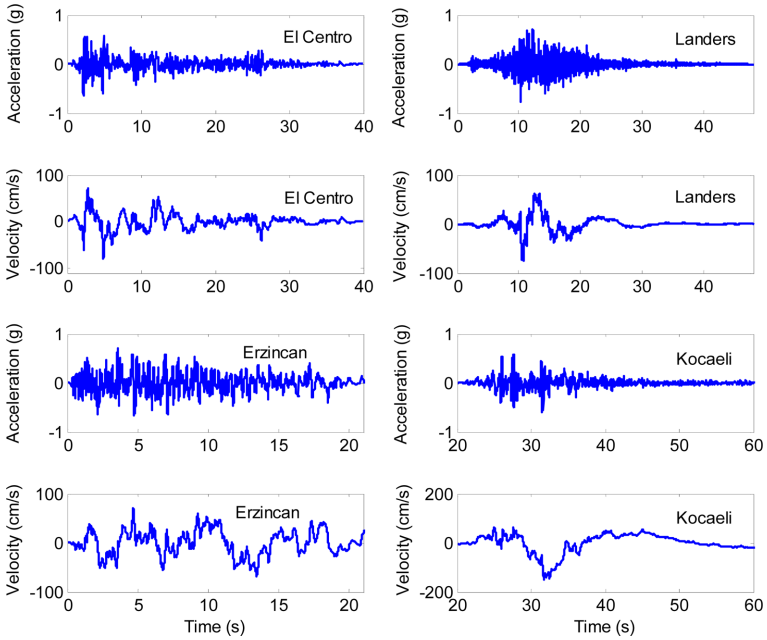

Fig. 3 Acceleration and velocity time-histories of ground motions used in analyses

(2×1) vector of restoring forces. Noting that $\{\mathbf{u_t}(t)\} = \{\mathbf{u}(t)\} + \{\mathbf{r}\}\mathbf{u_g}(t)$, where $\mathbf{u_g}(t)$ is the ground displacement and $\{\mathbf{r}\}$ is a vector coupling the direction of the ground motion input with the direction of the displacement, the equation of the motion given above can also be written as

$$\mathbf{M}\{\ddot{\mathbf{u}}_\mathbf{t}(t)\} + \mathbf{C}\{\dot{\mathbf{u}}_\mathbf{t}(t)\} + \mathbf{F_r}(t) = -\mathbf{M}\{\mathbf{r}\}\ddot{\mathbf{u}}_\mathbf{g}(t) \tag{6}$$

Integration of Eqs. (5) and (6) with respect to relative displacement $\{\mathbf{u}(t)\}$ over the entire duration of the seismic input leads to absolute and relative energy balance equations, respectively (Uang and Bertero 1990). Hence, the absolute energy balance equation of an isolated bridge can be written as

$$\frac{1}{2}\{\dot{\mathbf{u}}_\mathbf{t}(t)\}^T\mathbf{M}\{\dot{\mathbf{u}}_\mathbf{t}(t)\} + \int_0^t\{\dot{\mathbf{u}}_\mathbf{t}(t)\}^T\mathbf{C}\mathrm{d}\{\mathbf{u}(t)\} + \int_0^t\mathrm{d}\{\mathbf{u}_\mathbf{t}(t)\}^T\{\mathbf{F_r}(t)\} = \int_0^t\mathbf{M}\{\mathbf{r}\}^T\{\ddot{\mathbf{u}}_\mathbf{t}(t)\}\ddot{\mathbf{u}}_\mathbf{g}(t)\mathrm{d}t \tag{7}$$

Eq. (7) can be simply expressed as

$$E_K + E_\xi + E_A = E_I \tag{8}$$

where E_K denotes the absolute kinetic energy; E_ξ is the damping energy; E_A is the absorbed energy; which is the sum of the recoverable elastic strain energy E_S and the irrecoverable hysteretic energy E_H; and E_I represents the absolute input energy. Similarly, the relative energy equation of the isolated bridge can be written as follows

$$\frac{1}{2}\{\mathbf{u}_\mathbf{t}(t)\}^T\mathbf{M}\{\mathbf{u}_\mathbf{t}(t)\} + \int_0^t\{\dot{\mathbf{u}}_\mathbf{t}(t)\}^T\mathbf{C}\mathrm{d}\{\mathbf{u}(t)\} + \int_0^t\mathrm{d}\{\mathbf{u}(t)\}^T\{\mathbf{F_r}(t)\} = -\int_0^t\mathrm{d}\{\mathbf{u}(t)\}^T\mathbf{M}\{\mathbf{r}\}\ddot{\mathbf{u}}_\mathbf{g}(t) \tag{9}$$

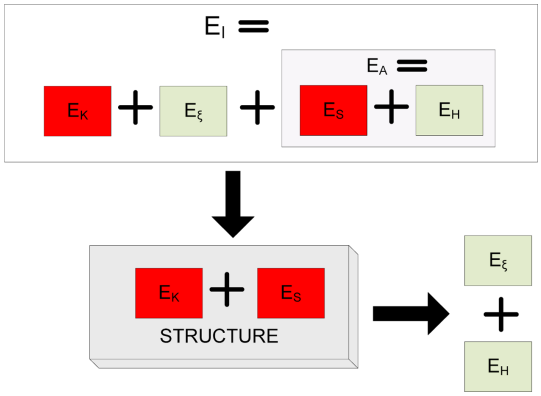

Fig. 4 Energy balance and energy exchange between structure and its environment

Fig. 4 shows a schematic representation of energy balance equation and energy exchange between structure and its environment. Note that the sum of the kinetic energy E_K and the strain energy E_S, called as recoverable energy, is stored within the structure and therefore should be minimized to prevent damages.

In previous studies, the absolute energy equation was used by some researchers to quantify the energy imparted to the structures (Park and Otsuka 1999, Chapman 1999, Takewaki 2004), while the relative energy formulation (Fajfar and Vidic 1994, Ordaz *et al.* 2003, Marano and Greco 2003, Takewaki and Fujita 2009) was employed by others. Kalkan and Kunnath (2008) investigated the relevance of using absolute and relative energy formulation in seismic evaluation of structures that are subjected to near-field ground motions. They found that the difference between absolute and relative energy input to structural systems during near-field earthquakes is much larger than that of in the case of far-field earthquakes. They suggested that selection of appropriate energy measure for near-field earthquakes should be based on the shape and period of the dominant pulse in the ground motion record and the vibration properties of the structural system. It was noted that arbitrarily using absolute or relative energy definitions for near-field ground motions can result in overlooking significant information.

In order to illustrate the difference in absolute and relative energy input to a structure during a typical far-field and near-field earthquake, Fig. 5 shows energy response history of the non-isolated

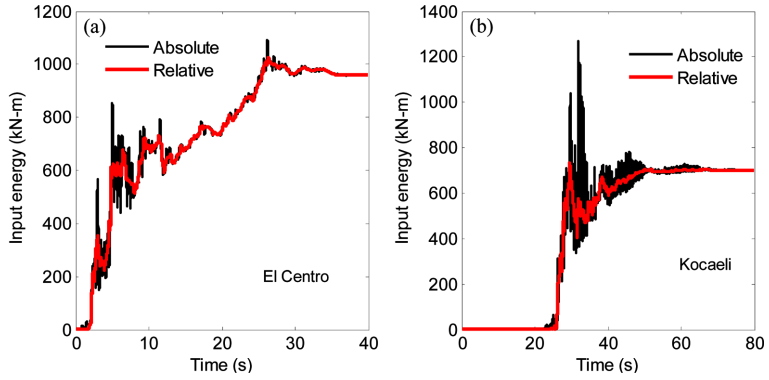

Fig. 5 Input energy time histories for a typical (a) far-field and (b) near-field earthquake

bridge subjected to a far-field (1940 El Centro) and a near-field (1999 Kocaeli) ground motion. It can be seen that the two different energy formulations result in similar input energy response histories for the far-field earthquake and input energy gradually builds up and reaches to a maximum near the end of the ground motion. In contrast, instantaneous energy spikes that have considerably larger values than the energy accumulated at the end are present in the response time history of the near-field earthquake. The values of absolute and relative input energy differ significantly during these energy spikes. Therefore, both absolute and relative energy balance formulations are considered to evaluate the energy response of the isolated bridge with SMA-based isolations systems subjected to different earthquakes in the next section.

3. Numerical study

In this section, an energy-based methodology is used to compare the performances of the S-FBI system and the SRB-IS for protecting bridge structures against various earthquakes. Fig. 6 shows the idealized force-displacement curve of a SMA device. In the figure, F_y and u_y represent forward transformation force and displacement of the SMA device; k_{SMA} and αk_{SMA} denote initial and post transformation stiffness of the device, respectively. For the NiTi wire considered in this study, α, which represents the ratio of post transformation stiffness and initial stiffness of the SMA device, is considered to be 0.1 and the forward transformation strain of SMA wire ε_y is about 1%. The forward transformation displacement u_y and the normalized forward transformation strength of the SMA device F_o are selected to characterize the SMA device of the smart isolation systems. Here, the forward transformation strength F_y is normalized by the weight of the bridge deck. Note that once u_y and F_y are given, the geometric dimensions of the SMA elements can be computed from

$$u_y = \varepsilon_y \cdot L_{SMA}$$
$$k_{SMA} = \frac{F_y}{u_y} = \frac{A_{SMA} \cdot E_{SMA}}{L_{SMA}} \tag{10}$$

where E_{SMA}, A_{SMA} and L_{SMA} are the Young's modulus, cross-sectional area and length of the SMA wires, respectively.

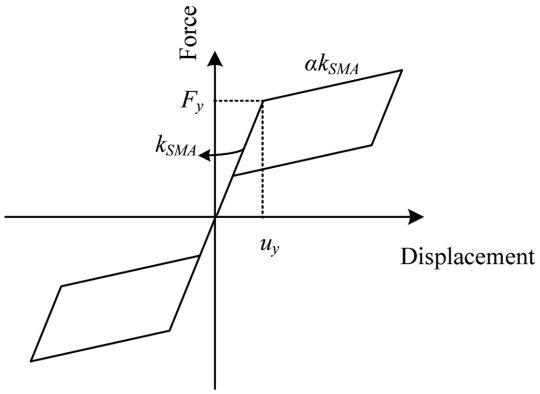

Fig. 6 Idealized force-displacement curve of SMA device

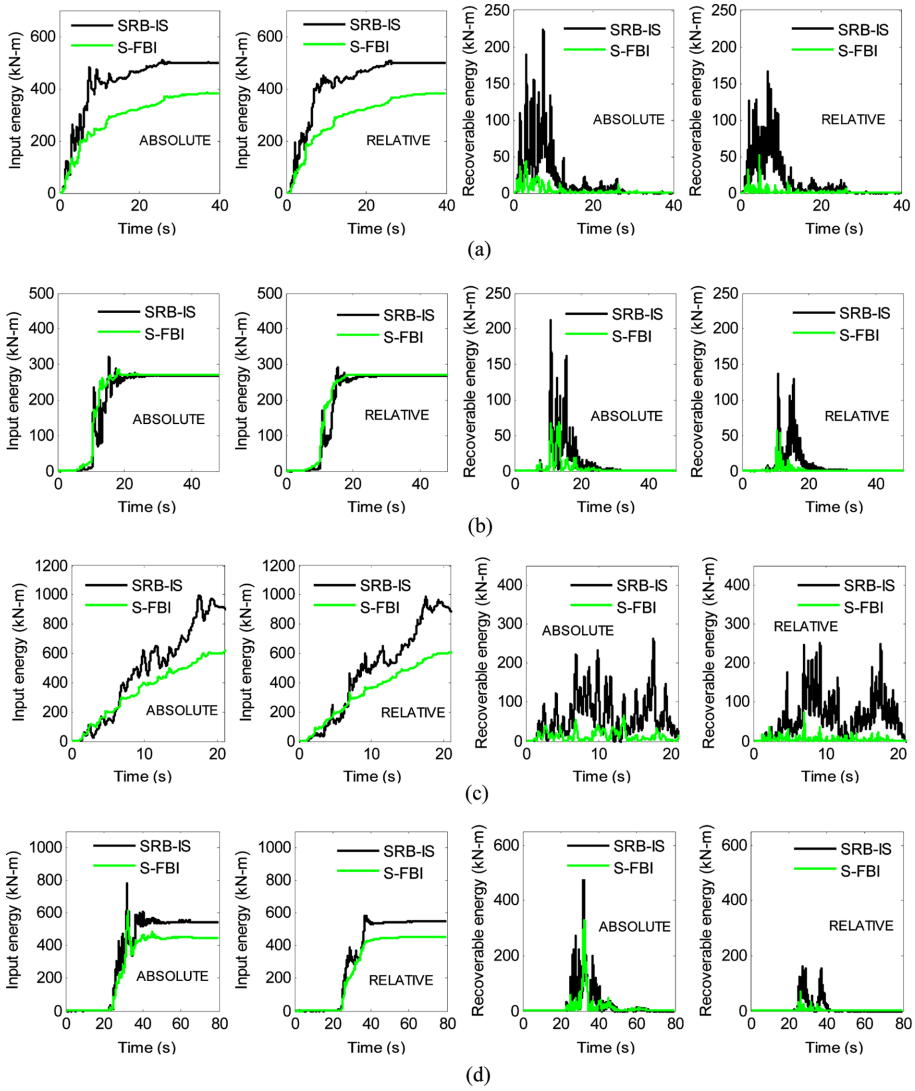

Fig. 7 Time histories of absolute and relative input energy and recoverable energy for (a) El Centro, (b) Landers, (c) Erzincan and (d) Kocaeli earthquakes

Based on the findings of Ozbulut and Hurlebaus (2011b), an optimal SRB-IS is designed with the parameters of $u_y = 40$ mm and $F_o = 0.20$ for the SMA device, and $k_b = 25$ kN/cm and 2% viscous damping ratio for the laminated rubber bearing. The optimum design parameters for the S-FBI system are adopted from Ozbulut and Hurlebaus (2011a). For this system, the flat sliding bearings has a friction coefficient of 0.10 and, the parameters of the SMA device are $u_y = 30$ mm and $F_o = 0.06$. Note that for the above design parameters, the volume of the SMA wires used in the S-FBI system is 70% less than the volume of the SMA material employed in the SRB-IS.

Fig. 7 shows the time histories of input energy and recoverable energy (kinetic energy + strain energy) for absolute and relative energy balance formulations for the isolated bridges subjected to the El Centro, Landers, Erzincan and Kocaeli earthquakes. It can be seen that absolute and relative

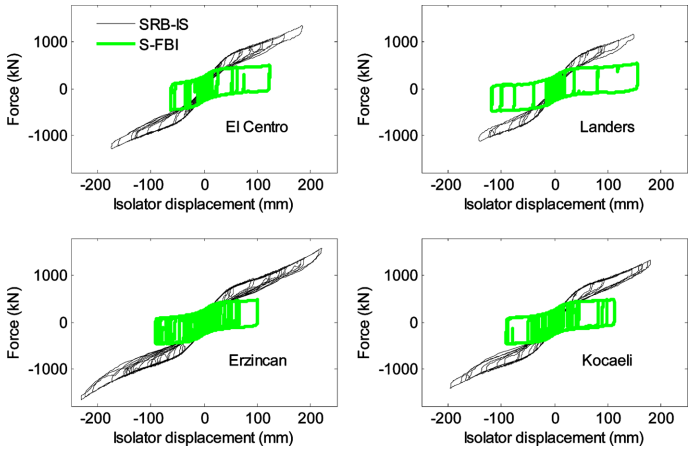

Fig. 8 Force-displacement curves of S-FBI and SRB-IS subjected to different excitation cases

input energy are very similar and cumulatively increase and reach a maximum at the end of the motion for both the S-FBI and SRB-IS for the El Centro earthquake. However, for some of the near-field earthquakes, energy spikes are observed especially in the absolute input energy at the early stages of the excitation. Specifically, the Kocaeli earthquake produces considerably high instantaneous absolute energy spikes for both isolation systems. It should be noted that the peak input energy, either computed through absolute or relative energy formulations, is smaller for the S-FBI system compared to the SRB-IS for all excitation cases.

When the time histories of recoverable energy transmitted to the bridge structure are compared, it can be seen that there is a substantial reduction in recoverable energy, which is the cause of the damage in the structure, for the S-FBI system in comparison with that of the SRB-IS. This is observed for all excitation cases and irrespective of absolute or relative energy formulation. The reason for the higher recoverable energy observed in the SRB-IS resides in the larger forces transmitted to the superstructure by the SRB-IS as compared to those transferred by the S-FBI system. This can be clearly seen from Fig. 8 that shows the force-displacement curves of both isolation systems subjected to different excitation cases.

The time histories of the deck drift and base shear normalized by the weight of the deck are given in Fig. 9 for different excitation cases. It can be seen that the S-FBI system reduces the peak deck drift considerably more than the SRB-IS when the isolated bridges subjected to El Centro, Erzincan and Kocaeli earthquakes. Both systems produce similar peak deck drift in the case of the Landers excitation. Also, the SRB-IS damps out the vibrations over longer time. The S-FBI system has consistently smaller peak base shear for the considered earthquakes. That is again due to the larger hysteretic force generated in the SRB-IS as shown in Fig. 8. Furthermore, both isolation systems recover all of their deformations at the end of the excitation. This implies there is no need for the replacement or refurbishment of the isolation system or its components and, the isolation system is ready for the service again for possible following earthquakes.

Fig. 10 illustrates the energy absorbed by the subcomponents of SMA-based isolation systems, i.e., the steel-Teflon bearings and the SMA device for the S-FBI system and, the rubber bearings and the SMA device for the SRB-IS. It can be seen that the energy is dissipated mainly by the SMA wires for the SRB-IS whereas the SMA device serves as a re-centering component in the S-

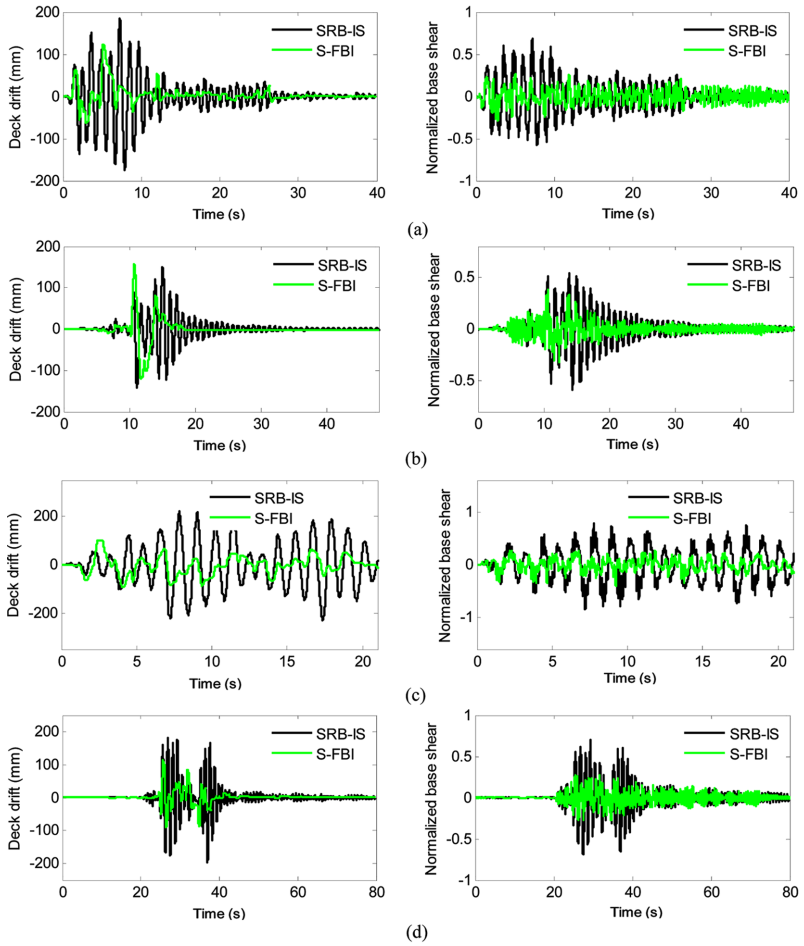

Fig. 9 Time histories of deck drift and normalized base shear for (a) El Centro, (b) Landers, (c) Erzincan and (d) Kocaeli earthquakes

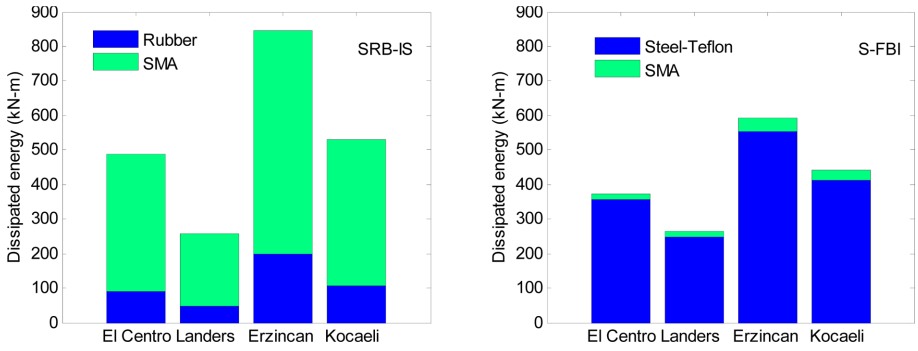

Fig. 10 Energy dissipated by the subcomponents of the (a) SRB-IS and (b) S-FBI

FBI system and the energy is dissipated through friction in the sliding surface for the S-FBI system. Since the energy dissipation in the SRB-IS relies primarily on the hysteretic behavior of the SMA

elements, the volume of the SMA wires employed in the SRB-IS is considerably higher than that used in the S-FBI system. As a result of larger amount of the SMA elements used in the SRB-IS, the force developed in the SRB-IS is higher than the restoring force of the S-FBI system.

4. Conclusions

This study compares the performances of two different SMA-based isolation systems, namely the S-FBI system and SRB-IS by conducting nonlinear time history analyses with energy balance assessment. First, absolute and relative energy balance equations are introduced for an isolated bridge structure. Then, a numerical study is performed to compare the response of a bridge structure isolated by an S-FBI system with that of an SRB-IS.

It is found that the bridge structure isolated by either the SRB-IS or the S-FBI system can effectively limit the peak deck drift response for considered excitations. However, it is noted that the peak base shear exhibits higher values in the case of the SRB-IS. When energy responses of the isolation systems are compared, it is observed that the S-FBI system attracts smaller quantities of input energy than the SRB-IS. The recoverable energy, which is the amount of the energy stored in the structure during the earthquake, is also considerably smaller for the S-FBI system as compared to the SRB-IS. It is shown that the energy is mainly dissipated by the SMA components for the SRB-IS. On the other hand, the energy dissipation in the S-FBI system is through friction, while the SMA component of the isolation system serves as a re-centering device. Since the energy dissipation in the SRB-IS almost solely depends on the hysteretic behavior of SMAs, and, the energy dissipation capabilities of the superelastic SMAs are limited, the larger amount of SMA material is required for the SRB-IS. To be more specific, the S-FBI system employs superelastic SMA wires that are 70% less in volume as compared to those used in the SRB-IS for the considered numerical example. Since the high cost of the SMAs is one of the main impediments that preclude the use of SMAs in a full-scale seismic application, requiring significantly less material gives an another advantage to the S-FBI system over the SRB-IS. Overall, it can be concluded that the S-FBI system which combines SMAs with flat sliding bearings has more favorable properties than the SRB-IS which consists of a laminated rubber bearing and a SMA device.

References

Attanasi, G., Auricchio, F. and Fenves, G. (2009), "Feasibility assessment of an innovative isolation bearing system with shape memory alloys", *J. Earthq. Eng*., **13**, 18-39.

Austin, M.A. and Lin, W.J. (2004), "Energy balance assessment of base isolated structures", *J. Eng. Mech. -ASCE*., **130**(3), 347-358.

Bruneau, M. (1998), "Performance of steel bridges during the 1995 Hyogoken-Nanbu (Kobe, Japan) earthquake-a North American perspective", *Eng. Struct*., **20**(12), 1063-1078.

Carreras, G., Casciati, F., Casciati, S., Isalgue, A., Marzi, A. and Torra, V. (2011), "Fatigue laboratory tests toward the design of SMA portico-braces", *Smart Struct. Syst*., **7**(1), 41-57.

Casciati, F. and Faravelli, L. (2009), "A passive control device with SMA components: From the prototype to the model", *Struct. Health Monit*., **16**(7-8), 751-765.

Casciati, F. and Lagorio, H.J. (1996), "Urban renewal aspects and technological devices in infrastructure

rehabilitation", *Proceedings of the 1st European Conference on Structural Control*, Barcelona, Spain, World Scientific Publishing Co., Ltd.
Casciati, S. and Marzi, A. (2010), "Experimental studies on the fatigue life of shape memory alloy bars", *Smart Struct. Syst*., **6**(1), 73-85.
Casciati, F. and van der Eijk, C. (2008), "Variability in mechanical properties and microstructure characterization of CuAlBe shape memory alloys for vibration mitigation", *Smart Struct. Syst*., **4**(2), 103-122.
Casciati, F. and Yao, T. (1995), "Comparison of strategies for the active control of civil structures", *Proceedings of the 1st World Conference on Structural Control*, (Eds. G. W. Housner, S. F. Masri, and A. G. Chassiakos), IASC, Los Angeles, CA, U.S.A., Vol. I, WA1-3.
Casciati, F., Faravelli, L. and Al Saleh. R. (2009), "An SMA passive device proposed within the highway bridge benchmark", *Struct. Health Monit*., **16**(6), 657-667.
Casciati, F., Faravelli, L. and Hamdaoui, K. (2007), "Performance of a base isolator with shape memory alloy bars", *Earthq. Eng. Eng. Vib*., **6**(4), 401-408.
Casciati, F., Faravelli, L. and Yao, T. (1996), "Control of nonlinear structures using the fuzzy control approach", *Nonlinear Dynam*., **11**(2), 171-187.
Chapman, M.C. (1999), "On the use of elastic input energy for seismic hazard analysis", *Earthq. Spectra*., **15**(4), 607-635.
Constantinou, M.C. and Reinhorn, A.M. (1995), "*Seismic isolation and control*", in Computer Analysis and Design of Earthquake Resistant Structures, Elsevier Applied Science, London.
Constantinou, M., Mokha, A. and Reinhorn, A. (1990), "Teflon bearing in base isolation II: Modeling", *J. Struct. Eng*., **116**(2), 455-74.
Dolce, M., Cardone, D. and Ponzo, F.C. (2007), "Shaking-table tests on reinforced concrete frames with different isolation systems", *Earthq. Eng. Struct. D*., **36**(5), 573-596.
Enke, D. L., Tirasirichai, C. and Luna, R. (2008), "Estimation of earthquake loss due to bridge damage in the St. Louis metropolitan area. II: Indirect losses", *Nat. Hazard Rev*., **9**(1), 12-19.
Fajfar, P. and Vidic, T. (1994), "Consistent inelastic design spectra: hysteretic and input energy", *Earthq. Eng. Struct. D*., **23**(5), 523-537.
Faravelli, L. and Yao, T. (1996), "Use of adaptive network in fuzzy control of civil structures", *Microcomput. Civil Eng*., **11**(1), 67-76.
Hancock, J., Bommer, J.J. and Stafford, P.J. (2008), "Numbers of scaled and matched accelerograms required for inelastic dynamic analyses", *Earthq. Eng. Struct. D*., **37**(14), 1585-1607.
Hancock, J., Watson-Lamprey, J., Abrahamson, N.A., Bommer, J.J., Markatis, A., McCoy, E. and Mendis, R. (2006), "An improved method of matching response spectra of recorded earthquake ground motion using wavelets", *J. Earthq. Eng*., **10**(1), 67-89.
Housner, G.W. (1956), "Limit design of structures to resist earthquakes", *Proceedings of the 1st World Conference on Earthquake Engineering*, Berkeley, CA, U.S.A.
Hsu, Y.T. and Fu, C.C. (2004), "Seismic effect on highway bridges in Chi Chi earthquake", *J. Perform. Constr. Fac*., **18**(1), 47-53.
Hurlebaus, S. and Gaul, L. (2006), "Smart structure dynamics", *Mech. Syst. Signal Pr*., **20**(2), 255-281.
IBC 2000 International Building Code International Code Council: Falls Church, VA, U.S.A.
Iervolino, I., Maddaloni, G. and Cosenza, E. (2009), "A note on selection of time- histories for seismic analysis of bridges in Eurocode 8", *J. Earthq. Eng*., **13**(8), 1125-1152.
Ismail, M., Rodellar, J. and Ikhouane, F. (2009). "An innovative isolation bearing for motion-sensitive equipment", *J. Sound. Vib*., **326**(3-5), 503-521.
Ismail, M., Rodellar, J. and Ikhouane, F. (2010), "An innovative isolation device for aseismic design", *Eng. Struct*., **32**(4), 1168-1183.
Jang, J.S.R. (1993), "ANFIS: Adaptive-network-based fuzzy inference system", *IEEE T. Syst, Man, Cy. B.,* **23**(3), 665-685.
Kalkan, E. and Kunnath, S.H. (2008), "Relevance of absolute and relative energy content in seismic evaluation of structures", *Adv. Struct. Eng*., **11**(1), 1-18.
Liu, Z. (2009), "Reconnaissance and preliminary observations of bridge damage in the great Wenchuan earthquake, China", *Struct. Eng. Int. J. Inter. Assoc. Bridge. Struct. Eng*., **19**(3), 277-282.

Malhotra, P.K. (2003), "Strong-motion records for site-specific analysis", *Earthq. Spectra*, **19**, 557-578.
Marano, G.C. and Greco, R. (2003), "Efficiency of base isolation systems in structural seismic protection and energetic assessment", *Earthq. Eng. Struct. D.*, **32**(10), 1505-1531.
Nezhad, H.T., Tait, M.J. and Drysdale, R.G. (2008), "Lateral response evaluation of fiber-reinforced neoprene seismic isolators utilized in an unbonded application", *J. Struct. Eng.*, **134**(10), 1627-1637.
Ordaz, M., Huerta, B. and Reinoso, E. (2003), "Exact computation of input-energy spectra from Fourier amplitude spectra", *Earthq. Eng. Struct. D.*, **32**(4), 597-605.
Ozbulut, O.E., Mir, C., Moroni, M.O., Sarrazin, M. and Roschke, P.N. (2007), "Fuzzy model of superelastic shape memory alloys for vibration control in civil engineering applications", *Smart Mater. Struct.*, **16**(3), 818-829.
Ozbulut, O.E. and Hurlebaus, S. (2010a), "Evaluation of the performance of a sliding-type base isolation system with a NiTi shape memory alloy device considering temperature effects", *Eng. Struct.*, **32**(1), 238-249.
Ozbulut, O.E. and Hurlebaus, S. (2010b), "Neuro-fuzzy modeling of temperature- and strain-rate dependent behavior of NiTi shape memory alloys for seismic applications", *J. Intell. Mater. Struct.*, **21**(8), 837-849.
Ozbulut, O.E. and Hurlebaus, S. (2011a), "Optimal design of superelastic-friction base isolators for seismic protection of highway bridges against near-field earthquakes", *Earthq. Eng.Struct. D.*, **40**(3), 273-291.
Ozbulut, O.E. and Hurlebaus, S. (2011b), "Seismic assessment of bridge structures isolated by a shape memory alloy/rubber-based isolation system", *Smart Mater. Struct.*, **20**(1), 015003.
Park, J.G. and Otsuka, H. (1999), "Optimal yield level of bilinear seismic isolation devices", *Earthq. Eng. Struct. D.*, **28**, 941-955.
Soong, T.T. and Constantinou, M.C. (1994), "*Passive and active structural vibration control in civil engineering*", Springer, New York, U.S.A.
Takewaki, I. (2004), "Bound of earthquake input energy", *J. Struct. Eng.*, **130**(9), 1289-1297.
Takewaki, I. and Fujita, K. (2009), "Earthquake input energy to tall and base-isolated buildings in time and frequency dual domains", *Struct. Des. Tall Spec.*, **18**(6), 589-606.
Uang, C.M. and Bertero, V.V. (1990), "Evaluation of seismic energy in structures", *Earthq. Eng. Struct. D.*, **19**(1), 77-90.
Usman, M., Sung, S.H., Jang, D.D., Jung, H.J. and Koo, J.H. (2009), "Numerical investigation of smart base isolation system employing MR elastomer", *J. Phys.*, **149**(1), 012099.
Wang, Y.P., Chung, L.L. and Liao W.H. (1998), "Seismic response analysis of bridges isolated with friction pendulum bearings", *Earthq. Eng. Struct. D.*, **27**(10), 1069-1093.
Wilde, K., Gardoni, P. and Fujino, Y. (2000), "Base isolation system with shape memory alloy device for elevated highway bridges", *Eng. Struct.*, **22**(3), 222-229.

FC